WDM Source Based on High-Power, Efficient 1280-nm DFB Lasers for Terabit Interconnect Technologies

Bob B. Buckley, Stewart T. M. Fryslie, Keith Guinn, *Senior Member, IEEE*, Gordon Morrison, *Member, IEEE*, Alexander Gazman, *Student Member, IEEE*, Yiwen Shen, Keren Bergman, *Fellow, IEEE*, Milan L. Mashanovitch, *Senior Member, IEEE*, and Leif A. Johansson, *Member, IEEE*

***Abstract*— We present a proof-of-concept eight-channel wavelength-division-multiplexed (WDM) source for future terabit interconnects based on a highly efficient laser array. The array is composed of novel, high-power DFB lasers with record electro-optical efficiency, operating at 1280 nm, with >250-mW laser output power and laser efficiencies of up to 36%. The eight-laser array, with ∼100-GHz channel spacing is optically butt-coupled to a planar lightwave circuit that consists of low-loss silicon nitride waveguides clad with silicon oxide for appropriate optical routing. Two types of optical routing are explored: 1) all 8 laser wavelengths are mixed and output into 10 channels via a star coupler and 2) the laser wavelengths are combined into a single output via an arrayed waveguide grating router. The mixed/combined light is then butt-coupled to a fiber array to output the WDM source signal into polarization preserving single-mode fibers. Improvements in insertion loss, particularly from optical butt coupling, will make this approach a viable option for efficient WDM light sources.**

***Index Terms*— Arrayed waveguide grating, DFB, optical interconnects, planar lightwave circuit, semiconductor lasers, star coupler, wavelength combiner, wavelength division multiplexing.**

I. Introduction

WAVELENGTH-DIVISION-MULTIPLEXED (WDM) data streams have been widely deployed in inter data center (DC) interconnects. In recent years, increased bandwidth demands within the DC due to the growth of machine-generated traffic have caused link capacity and spectral efficiency to become important concerns and potentially bottlenecks for intra-DC interconnects [1]. Using WDM sources for intra-DC networks can bring scalability in bandwidth density needed to meet terabit Ethernet requirements. New WDM networks based on wavelength switching can facilitate flexible architectures that allow sub-networks to be easily connected using additional wavelengths without laying more fibers, reducing wiring complexity and cabling costs [2]. This requires the use of WDM transceivers capable of high baud-rate with multilevel modulation.

Advances in Silicon Photonic (SiP) technology with co-optimized electronic circuitry have shown high-speed optical links at small foot-print and low-energy consumption [3]. Since silicon does not have a direct bandgap, there are two main solutions for the light sources: hybrid integration [4] and external coupling [5]. Hybrid sources have shown peak efficiency up to 14% and peak power up to 18 mW [6]. From advances in fiber coupling methods [7], efficient external laser sources can pave the way for cost competitive integrated SiP WDM transceivers.

In terabit-capable WDM interconnect networks, the laser sources can account for more than 30% of the link power budget [8]. This significant energy expense can be mitigated by using an architecture with an efficient high-power laser utilized as a central WDM source [9] in conjunction with passive [10] or active [11] optical power splitters. Furthermore, a centralized high-power WDM source for all the transceivers in the network allows for a localized thermoelectric cooler (TEC) design that can contribute to reducing transceiver control complexity and cost.

To address the need for high-power WDM sources, we have proposed and demonstrated a concept for an integrated multi-wavelength source for future terabit interconnect applications. One of two demonstrated methods in this letter consists of a high-efficiency, high-power DFB laser array butt-coupled to a star coupler, as illustrated in Figure 1. The star-coupler multiplexes the input laser array signal and distributes these to many output ports, each containing the light from all input sources. The star coupler is designed for low excess insertion loss, while producing many copies of the optical signal to feed several transceivers. In this manner, a single WDM source can be cost-shared between a multitude of terabit optical interconnects. Assuming 10 mW per optical channel power target, the required power from each source is several

Manuscript received July 27, 2018; revised August 28, 2018; accepted September 18, 2018. Date of publication October 1, 2018; date of current version November 15, 2018. This work was supported by the U.S. Department of Energy, Office of Science, under Award DE-SC0017172. *(Corresponding author: Bob B. Buckley.)*

B. B. Buckley, S. T. M. Fryslie, K. Guinn, G. Morrison, M. L. Mashanovitch, and L. A. Johansson are with Freedom Photonics, Santa Barbara, CA 93117 USA (e-mail: bbuckley@freedomphotonics.com).

A. Gazman, Y. Shen, and K. Bergman are with the Department of Electrical Engineering, Columbia University, New York, NY 10027 USA.

Color versions of one or more of the figures in this letter are available online at http://ieeexplore.ieee.org.

Digital Object Identifier 10.1109/LPT.2018.2872597

1041-1135 © 2018 IEEE. Personal use is permitted, but republication/redistribution requires IEEE permission.
See http://www.ieee.org/publications_standards/publications/rights/index.html for more information.

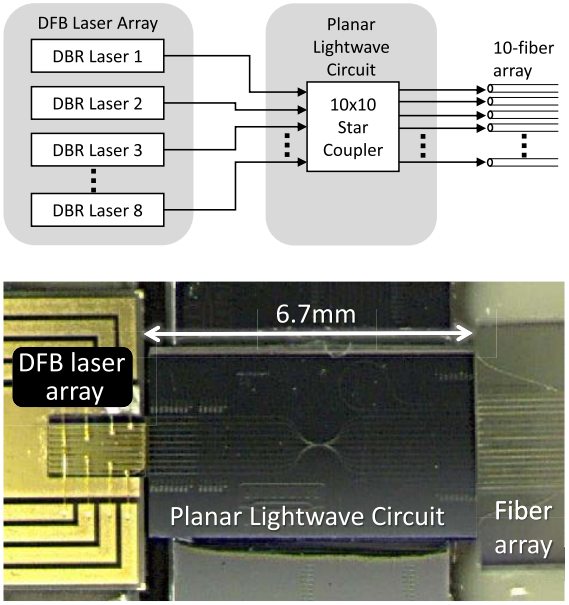

Fig. 1. Top – Diagram of 8-channel WDM source with 10 outputs. Bottom – Photo of assembled proof-of-concept demonstrator.

hundred mW, depending on output channel count. In our WDM source, we have utilized a novel, record efficiency, high power DFB laser array at 1280 nm, forming an 8-channel WDM source, coupled to a $10x10$ star coupler. The second method demonstrated for a WDM source uses an AWGR in place of the star coupler described above, to combine all 8 wavelengths into a single output for applications requiring increased power.

II. Efficient DFB Laser Array

A new DFB laser technology based on InGaAsP multi-quantum well active regions has been developed for high output power and high electro-optical efficiency. The DFB laser design was optimized for high efficiency, high output power following the design procedure described well in [12]. The epitaxial structure is designed with special attention to minimizing free-carrier absorption and voltage drop across the laser diode. The Bragg grating is designed using the methods in [13] considering the index contrast, thickness, and location with respect to the optical mode such that the combination of cavity length and coupling coefficient κ between the forward and backward propagating waves are optimized for single-mode lasing and reduced spatial hole burning, typically corresponding to κL value of $\sim$1 where L is the length of the laser cavity.

Figure 2 top shows the output power and efficiency for one particular laser implementation, where the back facet is high-reflectivity (HR) coated for improved front-facet efficiency. Peak electro-optical efficiency around 36% is observed at $\sim$4x threshold current, and peak power $>$ 200mW. Figure 2 bottom shows lasing spectra obtained at room temperature at different laser bias. Stable and highly single-mode emission is demonstrated.

For initial DFB laser array demonstration, we designed a 2 mm long by 1.2 mm wide laser array consisting of eight

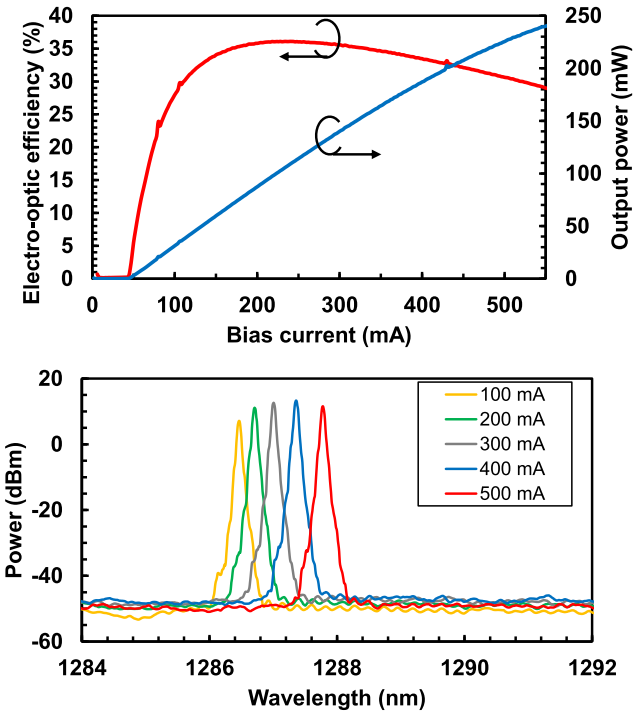

Fig. 2. Top - Output power and electro-optical efficiency of a single DFB laser. Back facet is HR coated such that the light primarily exits from the front facet and is detected. Bottom - Single-mode operation with laser bias. Data taken with temperature-controlled stage at 20°C.

DFB lasers placed on a single die at 127μm pitch, designed for 100 GHz wavelength spacing to form a source for an 8-channel WDM link. Figure 3 top shows the output power from a single DFB laser from this array biased individually. The peak output power exceeds 250 mW at $>$ 1A bias current. The peak efficiency at 700 mA bias current is $>$ 17% from a single anti-reflection (AR) coated facet, or $\sim$ 34% assuming symmetric emission from both AR coated facets, which is what is nominally expected. When all eight lasers are biased in parallel, $>$ 700mW of output power is generated at 4A bias current, as shown in Figure 3, bottom. Improved output power and efficiency from the laser bar can be expected through p-side down mounting, resulting in improved heat extraction and reduced junction temperatures, at the cost of increased alignment difficulty due to reduced visual references.

III. Star Coupler PLC WDM Source

For the source demonstrator, the anti-reflection (AR) coated 8-laser array is butt-coupled to an AR coated planar lightwave circuit (PLC) consisting of a $10x10$ star coupler fabricated using a low-loss nitride waveguide core buried in SiO_2. PLC Waveguides were optimized in geometry to remain single mode throughout the PLC routing, while minimizing bending loss, and matching laser and fiber modes at their respective facets via adiabatic tapers, as described in [14]. Device designs were optimized using finite difference time domain (FDTD) simulations.

Figure 4 top shows the simulated relative coupling efficiency from each laser to each output port of the star coupler. As can be observed, excluding the outermost ports, coupling loss is bound within a $\sim$ 3 dB range. Figure 4 bottom shows the

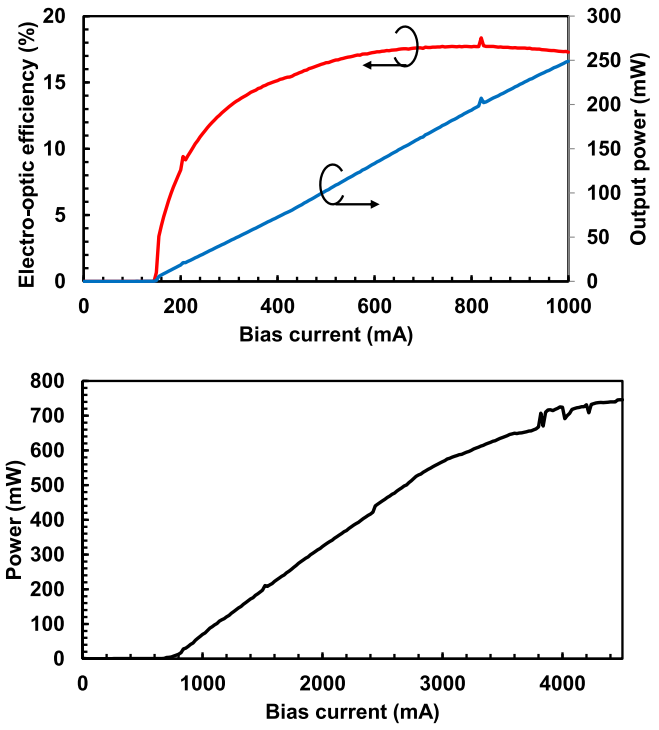

Fig. 3. Top - Output power and electro-optical efficiency for single DFB laser in the array out of the front facet. Bottom - Total output power for full 8-laser array biased in parallel when mounted p-side up, both taken at room temperature (20°C).

Simulated transmission

Fiber port

Laser port	A	B	C	D	E	F	G	H	I	J
A	40%	73%	79%	80%	78%	77%	77%	68%	44%	17%
B	44%	79%	87%	91%	91%	92%	91%	87%	68%	38%
C	53%	80%	91%	97%	98%	97%	96%	92%	77%	59%
D	62%	78%	91%	98%	100%	100%	98%	92%	77%	66%
E	66%	77%	92%	98%	100%	100%	98%	91%	78%	62%
F	59%	77%	92%	96%	98%	98%	96%	91%	81%	53%
G	39%	69%	87%	92%	92%	91%	91%	88%	79%	44%
H	17%	45%	69%	77%	77%	78%	81%	79%	74%	40%

Measured transmission

Fiber port

Laser port	A	B	C	D	E	F	G	H	I	J
A	16%	45%	45%	60%	78%	40%	56%	71%	51%	22%
B	15%	46%	77%	80%	81%	45%	63%	48%	63%	41%
C	23%	58%	80%	66%	84%	78%	70%	49%	52%	57%
D	52%	64%	63%	100%	93%	66%	89%	46%	57%	29%
E	30%	56%	73%	88%	89%	66%	56%	38%	51%	46%
F	54%	64%	77%	93%	98%	57%	72%	33%	56%	26%
G	40%	79%	74%	88%	86%	54%	53%	46%	66%	23%
H	16%	60%	81%	74%	71%	64%	47%	41%	44%	7%

Fig. 4. Top – FDTD Simulated relative coupling efficiency from each laser to each output port. Bottom - Measured relative coupling efficiency from each input port to each output port, before butt coupling to laser, using a tapered fiber to optically couple into the laser-end facet.

corresponding measured relative coupling efficiency from each laser to each output port, agreeing well with simulations. The absolute loss was measured between 19.6 dB and 23.4 dB, not including the outermost ports of the fiber array. This high coupling loss suggests the optical mode shape at the PLC facet was improperly matched to the laser and fiber optical modes. We expect further iterations of PLC designs would better match the laser and fiber optical modes, and that insertion loss could be improved to a 12-16 dB range for all output ports. A perfect NXN star coupler has an insertion loss of 1/N, or 10 dB in this case.

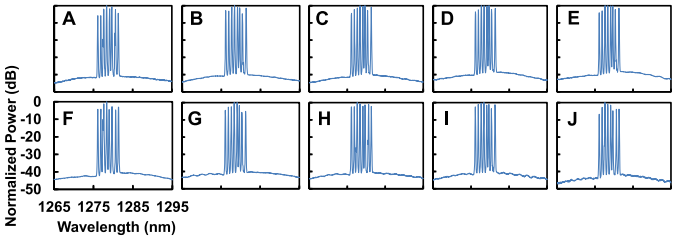

Fig. 5. Normalized optical spectra from each of the output ports of the star coupler (A-J), each port containing the signal from the combined WDM source. Data for all 10 ports are plotted on same scales.

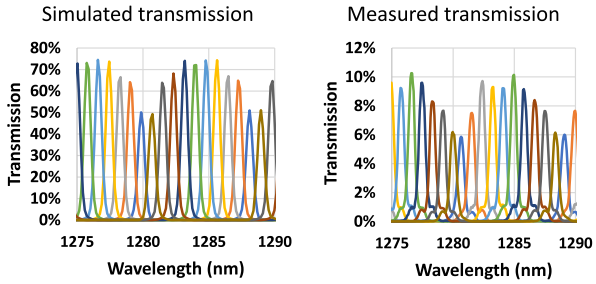

Fig. 6. Left – FDTD Simulated transmission spectra of an AWGR device. Right – Measured transmission of the AWGR, including insertion loss from aligned tapered fibers at input and output facets.

Figure 5 shows the resulting normalized optical spectra from each of the output ports of the star coupler, each port containing the signal from the combined WDM source. The variation in channel output power was limited by star coupler uniformity and input power from each laser. The laser array was designed for 100 GHz wavelength spacing. Measured average wavelength spacing was 112 GHz with 20 GHz deviation. Improved process control is expected to improve wavelength spacing and channel alignment.

IV. AWGR PLC WDM Source

Arrayed waveguide grating routers (AWGRs) were also designed and fabricated in our PLC platform, to combine all 8 wavelengths of the laser array into a single fiber, for maximum WDM laser source power in a single channel. AWGRs were designed with 10 input and 10 output ports such that all 8 lasers with appropriate wavelength spacing would exit the AWGR into a single fiber. Figure 6 shows the transmission spectra of all 10 input ports of an AWGR chip itself, both simulated (left) and measured (right). The absolute wavelength, wavelength spacing, and relative transmission between AWGR ports measured matches very well with what was theoretically expected in our device. The measured transmission also includes insertion loss from tapered fibers coupling light into and out of each port of the AWGR, and is thus $\sim$ 8.5 dB lower.

This AWGR was butt coupled to a laser array and fiber array similar to the star coupler. Figure 7 shows the laser array spectra for different output fibers of the laser array. One of the 8 lasers in the array was damaged, resulting in

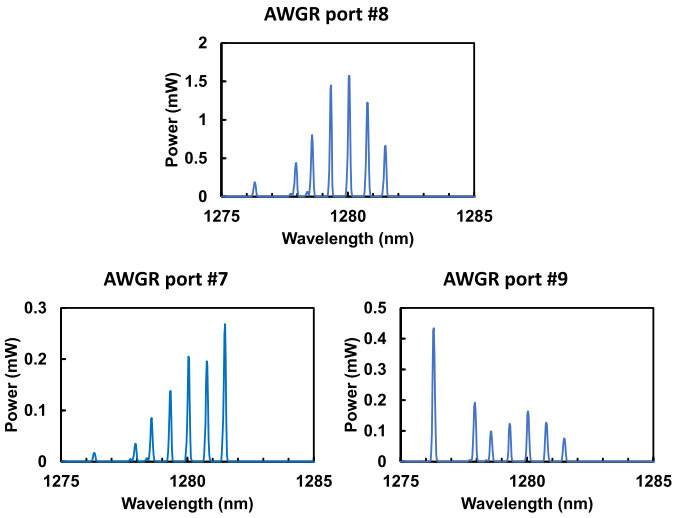

Fig. 7. Optical spectra of 3 adjacent output fiber ports of an AWGR coupled to a laser array. Most of the light from all lasers in the array exits into AWGR fiber port #8, while some light bleeds into ports #7 and #9.

output spectra of only 7 lasers. Most of the output power is combined into output port #8 of the $10x10$ AWGR. However, because the laser wavelength spacing and AWGR wavelength spacing is not perfectly aligned, the shorter-wavelength laser light also preferentially bleeds into output port #9, and the longer-wavelength lasers preferentially bleed into port #7. Better alignment of the relative wavelength spacing between lasers and the AWG will improve single-output alignment and loss due to light not aligned well with the AWGR output waveguide.

Loss measurements show roughly 4 dB insertion loss from butt coupling the lasers to PLC, an additional 4 dB of butt coupling loss from PLC to fiber array, 2.6 dB loss from light falling between output ports on the AWGR, and 2 dB loss from light exiting through the incorrect AWGR port. More closely matching the wavelength spacing between the laser array and AWGR would improve AWGR internal losses by $\sim$ 4.6 dB. In addition, improvements in PLC input/output mode matching with the lasers and fiber array optical modes would also improve butt coupling losses by several dB. Relative thermal drift between laser and PLC facets is a minimal effect, as expected for our package once properly aligned. We expect thermal gradients on the order of 10°C, the length scale of our package is $\sim$ 2 mm, and the coefficient of thermal expansion of our materials is on the order of $\sim$ 5e-6 /°C, resulting in possible thermal misalignments of $\sim$ 100 nm, which is 1 order of magnitude smaller than our mode size.

V. Conclusion

Future Si-photonics based terabit optical interconnects will require highly efficient and high power optical sources. In this letter, we have presented an integrated high power 1280 nm DFB laser array for this application. Single laser output power exceeds 250 mW, and the peak laser efficiency is 36%. A proof-of-concept integrated 8-channel WDM source is demonstrated with either 1 or 10 output ports, each containing a copy of the combined output from the efficient lasers. In addition, these high-power, high-efficiency DFB lasers could find use in other DC architectures which require high bandwidth communication with minimal power consumption.

Acknowledgment

This report was prepared as an account of work sponsored by an agency of the United States Government. Neither the United States Government nor any agency thereof, nor any of their employees, makes any warranty, express or implied, or assumes any legal liability or responsibility for the accuracy, completeness, or usefulness of any information, apparatus, product, or process disclosed, or represents that its use would not infringe privately owned rights. Reference herein to any specific commercial product, process, or service by trade name, trademark, manufacturer, or otherwise does not necessarily constitute or imply its endorsement, recommendation, or favoring by the United States Government or any agency thereof. The views and opinions of authors expressed herein do not necessarily state or reflect those of the United States Government or any agency thereof.

References

[1] L. Paraschis, "Advancements in data-center networking, and the importance of optical interconnections," in *Proc. 39th Eur. Conf. Exhib. Opt. Commun. (ECOC)*, London, U.K., Sep. 2013, pp. 1–3.

[2] H. Liu, C. F. Lam, and C. Johnson, "Scaling optical interconnects in datacenter networks opportunities and challenges for WDM," in *Proc. IEEE 18th Symp. High Perform. Interconnects*, Aug. 2010, pp. 113–116.

[3] L. Alloatti, "High-speed photonics for side-by-side integration with billion transistor circuits in unmodified CMOS processes," *J. Lightw. Technol.*, vol. 35, no. 6, pp. 1168–1173, Mar. 15, 2017.

[4] M. J. R. Heck and J. E. Bowers, "Energy efficient and energy proportional optical interconnects for multi-core processors: Driving the need for on-chip sources," *IEEE J. Sel. Topics Quantum Electron.*, vol. 20, no. 4, Jul./Aug. 2014, Art. no. 8201012.

[5] C.-H. Chen *et al.*, "A comb laser-driven DWDM silicon photonic transmitter based on microring modulators," *Opt. Express*, vol. 23, no. 16, pp. 21541–21548, 2015.

[6] B. R. Koch *et al.*, "Integrated silicon photonic laser sources for telecom and datacom," presented at the Opt. Fiber Commun. Conf., Anaheim, CA, USA, Mar. 2013.

[7] M. T. Wade *et al.*, "75% efficient wide bandwidth grating couplers in a 45 nm microelectronics CMOS process," in *Proc. IEEE Opt. Interconnects Conf. (OI)*, Apr. 2015, pp. 46–47.

[8] M. Bahadori, R. Polster, S. Rumley, Y. Thonnart, J.-L. Gonzalez-Jimenez, and K. Bergman, "Energy-bandwidth design exploration of silicon photonic interconnects in 65 nm CMOS," in *Proc. IEEE Opt. Interconnects Conf.*, May 2016, pp. 2–3.

[9] D. A. B. Miller, "Attojoule optoelectronics for low-energy information processing and communications," *J. Lightw. Technol.*, vol. 35, no. 3, pp. 346–396, Feb. 1, 2017.

[10] C. Sun *et al.*, "Single-chip microprocessor that communicates directly using light," *Nature*, vol. 528, no. 7583, pp. 534–538, Dec. 2015, doi: 10.1038/nature16454.

[11] A. Gazman, M. Bahadori, Z. Zhu, and K. Bergman, "Programmable optical power distribution in silicon photonic platform," in *Proc. IEEE Opt. Interconnects Conf. (OI)*, Jun. 2017, pp. 21–22.

[12] H. Wenzel *et al.*, "Design and realization of high-power DFB lasers," *Proc. SPIE*, vol. 5594, pp. 110–123, Dec. 2004.

[13] G. B. Morrison and D. T. Cassidy, "A probability-amplitude transfer matrix model for distributed-feedback laser structures," *IEEE J. Quantum Electron.*, vol. 36, no. 6, pp. 633–640, Jun. 2000.

[14] K. Shang, S. Pathak, C. Qin, and S. J. B. Yoo, "Low-loss compact silicon nitride arrayed waveguide gratings for photonic integrated circuits," *IEEE Photon. J.*, vol. 9, no. 5, Sep. 2017, Art. no. 6601805.